Preprints of the 21st IFAC World Congress (Virtual)
Berlin, Germany, July 12-17, 2020

Adaptive Output Feedback Controller of Voltage Source Inverters in Microgrid Connected Mode

L. Ammeh[1*], H. El Fadil[2], M. Oulcaid[3], F. Giri[4], T. Ahmed-Ali[5]

Automatic laboratory, Caen University, Normandie, France
(e-mails: [1]ammeh.leila@gmail.com, [2]elfadilhassan@yahoo.fr, [3]oulcaid02@gmail.com, [4]fouadgiri@yahoo.fr, [5]tarek.ahmed-ali@ensicean.fr)

Abstract: This paper deals with the control of Voltage Source Inverters (VSIs) connected to the main grid. The controller aim is fourfold: i) enforcing the current injected by the VSI to follow a given reference, ii) estimating the grid resistance and inductance, iii) estimating the current load and the grid voltage, iv) assuming an asymptotic stability of the system. To achieve these aims, we designed an adaptive output feedback controller using the backstepping technique and the high gain approach. Moreover, the controller has the ability to compensate the reactive power of the local load. The system stability was analyzed by Lyapunov theory. The controller performances were illustrated by simulations with grid parameter and load current variations.

Keywords: Adaptive output feedback control, voltage source inverter, microgrid connected mode, backstepping, high gain, adaptive control.

1. INTRODUCTION

In last years, Distributed Generation (DG) has become an interesting research topic. This rising interest is motivated by DG benefits; it reduces emissions and mitigates the climate changes, in another hand, it helps to meet the world power demand and limit the depletion of fossil fuel reserves. However, the use of an individual DG unit may cause many serious problems, local voltage rise is an example. To overcome these problems, the concept of microgrids stands as the best solution (Abdmouleh et al., 2017, Zamora and Srivastava, 2010, Mariam et al., 2013).

A microgrid is the combination of many DG units, storage systems and loads. A microgrid is a single controllable entity that can provide both power and heat to its local area (Hirsch et al., 2018). It has two operating modes; connected to the utility grid or autonomously. The transition between these two modes is ensured by a switching device at the point of common coupling (PCC).

Many DG units provide DC current while a lot of critical loads require AC current. Besides, to be connected to the main network, microgrids need Voltage Source Inverters (VSIs) to ensure the DC to AC electricity conversion. In connected mode the voltage amplitude and frequency are dictated by the utility grid, the VSI controls the injected current. While in islanded mode, the VSI has to control voltage and frequency at the PCC. In literature many techniques have been employed to control VSIs.

Proportional Integral (PI) and Proportional Integral Derivative (PID) controllers were used for regulating grid current (Siddique et al, 2019). These controllers are easy to be implemented and have good transient response. But the aforementioned performances are not achieved in the presence of unbalanced disturbances quantities (Hossain et al., 2017). In (Komurcugil et al., 2016), a Proportional Resonant (PR) controller was employed to regulate the current of a grid connected VSI. When it is used to control a sinusoidal waveform, it allows achieving a zero steady state error. This capability can be explored for harmonic compensation in microgrids. However, PR controller is sensitive to grid frequency variation and its parameters require to be accurately tuned (Hornik et al., 2011, Hossain et al., 2017). Model predictive control (MPC) was used for controlling current in microgrids (Calle-Prado et al., 2015, Hu et al., 2013). This controller predicts the system future behaviour on the base the present system state. It has the advantage of considering the system non linearities and constraints, reducing switching frequency and achieving an accurate current control. Though, MPC is highly sensitive to parameter changes. It requires a lot of calculations and an exact model of the filter (Bouzid et al., 2015).

In our paper we propose a controller for VSI in microgrid grid tied mode. This controller regulates the current injected by the VSI into the main grid in order to ensure the active and reactive power control. Furthermore, it has the ability to estimate the grid resistance and inductance. The VSI controllers require continuously the measurement of the system state. This measurement should be reliable to ensure satisfying results. However, in many cases the presence of noise and disturbances, it may not be possible to have reliable measurements and exact information. For these reasons, we improve our controller by designing a high gain observer which estimates the grid voltage as well as the load current.

The paper structure is the following: section 2 describes the studied system, section 3 presents the controller design, the observer design is given in section 4, section 5 studies the system global stability, section 6 shows simulation results and discussion before giving the conclusion and the references.

2. SYSTEM OVERVIEW AND MODELLING

The considered system is shown in Fig. 1. It comprises a standard three-phase VSI fed by a constant voltage DC bus. Its AC side is connected to an LC filter. The connection to the grid is released through an inductor representing the line impedance.

From Fig. 1 and applying Kirchhoff's voltage and current laws to the system single phase, the VSI current i_{in}, the voltage at the PCC v_{out} across the capacitor C and the output current i_{out} are given by (1)-(3).

$$\frac{di_{in}}{dt} = -\frac{R_1}{L_1} i_{in} + \frac{1}{L_1}(v_{in} - v_{out}) \tag{1}$$

$$\frac{dv_{out}}{dt} = \frac{1}{C}(i_{in} - i_{out} - i_{load}) \tag{2}$$

$$\frac{di_{out}}{dt} = -\frac{R_2}{L_2} i_{out} + \frac{1}{L_2}(v_{out} - v_{grid}) \tag{3}$$

Where L_1, R_1 and C are, respectively, the LC filter inductance, resistance and capacitance. v_{in} is the inverter output voltage. v_{grid} is the main grid voltage. i_{load} is the current load. L_2 and R_2 are the inductance and resistance of the line impedance. v_{out} and i_{out} are the output voltage and current at the PCC.

To handle with the VSI three phase model, we used a dq frame that rotates synchronously with the system output voltage angular speed ω_o at the PCC and we use state-space averaging. Hence, the mathematical model of the considered system in Fig. 2 is represented by (4)-(9)

$$\dot{x}_1 = -\frac{R_1}{L_1} x_1 + \omega_o x_2 - \frac{1}{L_1} x_3 + \frac{1}{L_1}\mu_1 \tag{4}$$

$$\dot{x}_2 = -\omega_o x_1 - \frac{R_1}{L_1} x_2 - \frac{1}{L_1} x_4 + \frac{1}{L_1}\mu_2 \tag{5}$$

$$\dot{x}_3 = \frac{1}{C}(x_1 - x_5 - i_{loadd}) + \omega_o x_4 \tag{6}$$

$$\dot{x}_4 = \frac{1}{C}(x_2 - x_6 - i_{loadq}) - \omega_o x_3 \tag{7}$$

$$\dot{x}_5 = \theta_1(x_3 - V_{gd}) - \theta_2 x_5 + \omega_o x_6 \tag{8}$$

$$\dot{x}_6 = \theta_1(x_4 - V_{gq}) - \theta_2 x_6 - \omega_o x_6 \tag{9}$$

Where $\theta_1 = \frac{1}{L_2}$, $\theta_2 = \frac{R_2}{L_2}$ (10)

The state vector $x = [i_{ind}, i_{inq}, v_{outd}, v_{outq}, i_{outd}, i_{outq}]^T$

The input vector $\mu = [v_{ind}, v_{inq}]^T$

The output vector $y = [v_{outd}, v_{outq}, i_{outd}, i_{outq}]^T$

V_{gd}, V_{gq}, i_{loadd} and i_{loadq} are the direct and quadrature components of the average values of grid voltage and the load current.

3. CONTROLLER DESIGN

The objective in this section is enforcing the output current to follow a given reference and estimating the grid resistance and inductance at the same time. To achieve this objective, we apply the adaptive backstepping technique.

First, we start by the direct component i_{outd} (x_5) of the output current i_{out}. Its reference is x_5^{ref}.

Step 1: We define the tracking error

$$e_1 = x_5 - x_5^{ref} \tag{11}$$

The dynamics of e_1 are given by

$$\dot{e}_1 = \theta_1(x_3 - V_{gd}) - \theta_2 x_5 + \omega_o x_6 - \dot{x}_5^{ref} \tag{12}$$

Let us define

$$\begin{aligned} \tilde{\theta}_1 &= \theta_1 - \hat{\theta}_1 \\ \tilde{\theta}_2 &= \theta_2 - \hat{\theta}_2 \end{aligned} \tag{13}$$

$\hat{\theta}_1$ and $\hat{\theta}_2$ are, respectively, θ_1 and θ_2 estimates.

e_1 vanishes if $\hat{\theta}_1 x_3 = \alpha_1$ where α_1 is a stabilizing function

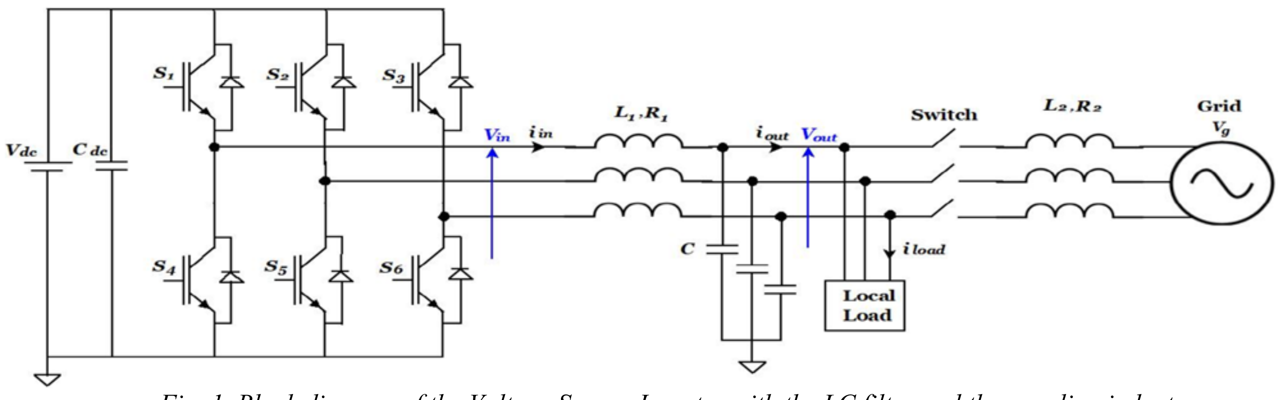

Fig. 1. Block diagram of the Voltage Source Inverter with the LC filter and the coupling inductor

given by (14).

$$\alpha_1 = -k_1 e_1 + \hat{\theta}_1 V_{gd} + \hat{\theta}_2 x_5 - \omega_o x_6 + \dot{x}_5^{ref} \tag{14}$$

With $k_1 \rangle 0$ is a design parameter.

The real control input does not appear by deriving the error e_1 and $\hat{\theta}_1 x_3$ is the virtual input. Then, we introduce a second tracking error e_2 defined as

$$e_2 = \hat{\theta}_1 x_3 - \alpha_1 \tag{15}$$

Step 2: let us differentiate (15) to find the dynamics of e_2.

$$\dot{e}_2 = \frac{\hat{\theta}_1}{C} x_1 + k_1 e_2 - k_1^2 e_1 + \varphi_1 + \beta_1 \tilde{\theta}_1 + \beta_2 \tilde{\theta}_2 \tag{16}$$

Where

$$\begin{aligned}
&\varphi_1 = \varphi_2 + \varphi_3 x_5 - 2\omega_o \hat{\theta}_2 x_6 - \ddot{x}_5^{ref} \\
&\varphi_2 = \dot{\hat{\theta}}_1 (x_3 - V_{gd}) + \hat{\theta}_1 [2\omega_o x_4 - \frac{i_{loadd}}{C} \\
&-\dot{V}_{gd} - \hat{\theta}_2 (x_3 - V_{gd}) - \omega_o V_{gq}] \\
&\varphi_3 = \frac{-\hat{\theta}_1}{C} - \dot{\hat{\theta}}_2 + \hat{\theta}_2^2 - \omega_o^2 \\
&\beta_1 = (k_1 - \hat{\theta}_2)(x_3 - V_{gd}) + \omega_o x_6 \\
&\beta_2 = x_5 (\hat{\theta}_2 - k_1) - \omega_o x_6
\end{aligned} \tag{17}$$

The error e_2 vanishes if $(\hat{\theta}_1 / C) x_1 = \alpha_2$. α_2 is the stabilizing function associated to the virtual control input $(\hat{\theta}_1 / C) x_1$.

$$\alpha_2 = e_1 (k_1^2 - 1) - e_2 (k_1 + k_2) - \varphi_1 \tag{18}$$

With $k_2 \rangle 0$ is a design parameter.

To ensure the convergence of e_1 and e_2 to zero, we define a third error tracking e_3 as

$$e_3 = (\hat{\theta}_1 / C) x_1 - \alpha_2 \tag{19}$$

If e_3 vanishes then e_2 vanishes. As a result, e_1 vanishes in its turn which is our objective.

Step3: Differentiating e_3, we get

$$\begin{aligned}
\dot{e}_3 = &\frac{\hat{\theta}_1}{CL_1} \mu_1 + e_1 (k_1^3 - 2k_1 - k_2) + e_2 (-k_1^2 - k_2^2 - k_1 k_2 + 1) \\
&+ e_3 (k_1 + k_2) + \varphi_4 + \beta_3 \tilde{\theta}_1 + \beta_4 \tilde{\theta}_2
\end{aligned} \tag{20}$$

Where

$$\begin{aligned}
&\varphi_4 = \frac{\dot{\hat{\theta}}_1}{C} x_1 + \frac{\hat{\theta}_1}{C} (-\frac{R_1}{L_1} x_1 + \omega_o x_2 - \frac{x_3}{L_1}) + \dot{\varphi}_2 \\
&+ \varphi_3 [\hat{\theta}_1 (x_3 - V_{gd}) - \hat{\theta}_2 x_5 + \omega_o x_6] - 2\omega_o \hat{\theta}_2 \\
&[\hat{\theta}_1 (x_4 - V_{gq}) - \hat{\theta}_2 x_6 - \omega_o x_6] + \dot{\varphi}_3 x_5 - 2\omega_o \dot{\hat{\theta}}_2 x_6 - \dddot{x}_5^{ref} \\
&\beta_3 = (x_3 - V_{gd})(1 - k_1^2 + \varphi_3) + \beta_1 (k_1 + k_2) - 2\omega_o \hat{\theta}_2 (x_4 - V_{gq}) \\
&\beta_4 = x_5 (k_1^2 - 1 - \varphi_3) + \beta_2 (k_1 + k_2) + 2\omega_o \hat{\theta}_2 x_6
\end{aligned} \tag{21}$$

Let us consider the following Lyapunov function candidate

$$V_1 = \frac{1}{2} \sum_{i=1}^{3} e_i^2 + \frac{1}{2\gamma_1} \tilde{\theta}_1^2 + \frac{1}{2\gamma_2} \tilde{\theta}_2^2 \tag{22}$$

$\gamma_1 \rangle 0$ and $\gamma_2 \rangle 0$ are parameter adaptation gains. They can be freely chosen.

Its time derivative is given by (23).

$$\begin{aligned}
\dot{V}_1 = &-k_1 e_1^2 - k_2 e_2^2 + e_3 [\frac{\hat{\theta}_1}{CL_1} \mu_1 + e_1 (k_1^3 - 2k_1 - k_2) \\
&+ e_2 (-k_1^2 - k_2^2 - k_1 k_2 + 1) + e_3 (k_1 + k_2) + \varphi_4] \\
&- \frac{\tilde{\theta}_1}{\gamma_1} \left[\dot{\hat{\theta}}_1 - \gamma_1 e_1 (x_3 - V_{gd}) - \gamma_1 e_2 \beta_1 - \gamma_1 e_3 \beta_3 \right] \\
&- \frac{\tilde{\theta}_2}{\gamma_2} \left[\dot{\hat{\theta}}_2 + \gamma_2 e_1 x_5 - \gamma_2 e_2 \beta_2 - \gamma_2 e_3 \beta_4 \right]
\end{aligned} \tag{23}$$

To eliminate $\tilde{\theta}_1$ and $\tilde{\theta}_2$ from $\dot{V}_1$, (24) define the parameter adaptive laws

$$\begin{aligned}
&\dot{\hat{\theta}}_1 = \gamma_1 \left[e_1 (x_3 - V_{gd}) + e_2 \beta_1 + e_3 \beta_3 \right] \\
&\dot{\hat{\theta}}_2 = \gamma_2 \left[-e_1 x_5 + e_2 \beta_2 + e_3 \beta_4 \right]
\end{aligned} \tag{24}$$

The control input law μ_1 is chosen as

$$\begin{aligned}
\mu_1 = &\frac{CL_1}{\hat{\theta}_1} [-e_1 (k_1^3 - 2k_1 - k_2) - e_2 (-k_1^2 - k_2^2 - k_1 k_2 + 2) \\
&- e_3 (k_1 + k_2 + k_3) - \varphi_4]
\end{aligned} \tag{25}$$

$k_3 \rangle 0$ is a design parameter.

Now, we follow the same approach and we apply the same steps to enforce i_{outq} (x_6) to track its reference. We get:

$$\begin{aligned}
\mu_2 = &\frac{CL_1}{\hat{\theta}_1} [-e_4 (k_4^3 - 2k_4 - k_5) - e_5 (-k_4^2 - k_5^2 - k_4 k_5 + 2) \\
&- e_6 (k_4 + k_5 + k_6) - \varphi_5]
\end{aligned} \tag{27}$$

The adaptive laws become:

$$\begin{aligned}
&\dot{\hat{\theta}}_1 = \gamma_1 [e_1 (x_3 - V_{gd}) + e_2 \beta_1 + e_3 \beta_3 \\
&+ e_4 (x_4 - V_{gq}) + e_5 \beta_5 + e_6 \beta_7] \\
&\dot{\hat{\theta}}_2 = \gamma_2 \left[-e_1 x_5 + e_2 \beta_2 + e_3 \beta_4 - e_4 x_6 + e_5 \beta_6 + e_6 \beta_8 \right]
\end{aligned} \tag{28}$$

Where

$$\begin{aligned}
&\varphi_5 = \frac{\dot{\hat{\theta}}_1}{C} x_2 + \frac{\hat{\theta}_1}{C} (-\frac{R_1}{L_1} x_2 - \omega_o x_1 - \frac{x_4}{L_1}) + \dot{\varphi}_6 \\
&+ \varphi_3 [\hat{\theta}_1 (x_4 - V_{gq}) - \hat{\theta}_2 x_6 - \omega_o x_5] + 2\omega_o \hat{\theta}_2 [\hat{\theta}_1 (x_3 - V_{gd}) \\
&- \hat{\theta}_2 x_5 + \omega_o x_5] + \dot{\varphi}_3 x_6 + 2\omega_o \dot{\hat{\theta}}_2 x_5 - \dddot{x}_6^{ref} \\
&\varphi_6 = \dot{\hat{\theta}}_1 (x_4 - V_{gq}) + \hat{\theta}_1 [-2\omega_o x_3 - \frac{i_{loadq}}{C} - \dot{V}_{gq} \\
&- \hat{\theta}_2 (x_4 - V_{gq}) + \omega_o V_{gd}] \\
&\beta_5 = (k_4 - \hat{\theta}_2)(x_4 - V_{gq}) - \omega_o x_5 \\
&\beta_6 = x_6 (\hat{\theta}_2 - k_4) + \omega_o x_5 \\
&\beta_7 = (x_4 - V_{gq})(1 - k_4^2 + \varphi_3) \\
&+ \beta_5 (k_4 + k_5) + 2\omega_o \hat{\theta}_2 (x_3 - V_{gd}) \\
&\beta_8 = x_6 (k_4^2 - 1 - \varphi_3) + \beta_6 (k_4 + k_5) - 2\omega_o \hat{\theta}_2 x_5
\end{aligned} \tag{29}$$

$k_4 \rangle 0,\ k_5 \rangle 0,\ k_6 \rangle 0$ are design parameters.

All the design parameters are freely chosen and they must be sufficiently large to reduce the tracking errors.

The system can be represented in a compact way as

$$\dot{e} = Ae + W^T \tilde{\theta} \tag{30}$$

$$\dot{\tilde{\theta}} = -\Gamma W e \tag{31}$$

Where

$e = \begin{bmatrix} e_1 & e_2 & e_3 & e_4 & e_5 & e_6 \end{bmatrix}^T, \theta = \begin{bmatrix} \theta_1 & \theta_2 \end{bmatrix}^T, \Gamma = \begin{bmatrix} \gamma_1 & \gamma_2 \end{bmatrix}$

$$A = \begin{bmatrix} -k_1 & 1 & 0 & 0 & 0 & 0 \\ -1 & -k_2 & 1 & 0 & 0 & 0 \\ 0 & -1 & -k_3 & 0 & 0 & 0 \\ 0 & 0 & 0 & -k_4 & 1 & 0 \\ 0 & 0 & 0 & -1 & -k_5 & 1 \\ 0 & 0 & 0 & 0 & -1 & -k_6 \end{bmatrix},$$

$$W = \begin{bmatrix} x_3 - V_{gd} & \beta_1 & \beta_3 & x_4 - V_{gq} & \beta_5 & \beta_7 \\ -x_5 & \beta_2 & \beta_4 & -x_6 & \beta_6 & \beta_8 \end{bmatrix}$$

4. HIGH OBSERVER DESIGN

In this section, we aim to observe the grid voltage and the current load which are unknown and variable. The observer is implemented on the base of the high gain approach presented in (Farza et al. 2004). This approach has the benefit to be simple but it requires a good choice of the design parameter; indeed, the choice of its single design parameter is a trade-off between the fast convergence and the sensitivity to noise. For a satisfying convergence the design parameter value should be high enough (Chaabane et al., 2014).

The system (4)-(9) could be written under the form in (32).

$$\begin{aligned} \dot{z} &= F(z)z + G(z,s) + \tilde{\xi}(t) \\ y &= \bar{B}z \end{aligned} \tag{32}$$

Where

$z = \begin{bmatrix} z^1 & z^2 \end{bmatrix}^T, z^1 = \begin{bmatrix} x_3 & x_4 & x_5 & x_6 \end{bmatrix}^T, s = \begin{bmatrix} x_1 & x_2 \end{bmatrix}^T$

$z^2 = \begin{bmatrix} i_{loudd} & i_{loadq} & V_{gd} & V_{gq} \end{bmatrix}^T, \dot{z}^2 = \xi(t),$

$\xi(t) = \begin{bmatrix} \xi_1 & \xi_2 & \xi_3 & \xi_4 \end{bmatrix}^T, \qquad \tilde{\xi}(t) = \begin{bmatrix} 0 & \xi(t) \end{bmatrix}^T,$

$F(z) = \begin{bmatrix} 0 & F_1(z) \\ 0 & 0 \end{bmatrix}, F_1(z) = diag(-\frac{1}{C}, -\frac{1}{C}, -\frac{1}{L_2}, -\frac{1}{L_2}),$

$\bar{B} = [I_4, 0_{4\times 4}], G(z,s) = \begin{bmatrix} G^1(z,s) & 0 \end{bmatrix}^T,$

$G^1(z^1, s) = [\frac{x_1 - x_5}{C} + \omega_o x_4, \frac{x_2 - x_6}{C} - \omega_o x_3,$

$\frac{x_3 - R_2 x_5}{L_2} + \omega_o x_6, \frac{x_4 - R_2 x_6}{L_2} - \omega_o x_5]^T$,

The observer is given by equation (33).

$$\dot{\hat{z}} = F(\hat{z})\hat{z} + G(s,\hat{z}) - \lambda \Lambda^+(s,\hat{z}) \Delta_\lambda^{-1} S_1^{-1} B^T \bar{B}(\hat{z} - z) \tag{33}$$

Where

λ is a real number, $\Lambda(s,\hat{z}) = diag\left[I_4, F_1(s,\hat{z})\right]$, $\Lambda^+(s,\hat{z})$ is the left inverse of $\Lambda(s,\hat{z})$.

$\Delta_\lambda = diag\left[I_4, \frac{1}{\lambda} I_4\right],\ S_1^{-1} B^T = \begin{bmatrix} 2I_4 \\ I_4 \end{bmatrix}$

As a consequence

$$\begin{aligned}
\dot{\hat{x}}_3 &= \frac{x_1 - \hat{x}_5 - \hat{i}_{loudd}}{C} + \omega_o \hat{x}_4 - 2\lambda(\hat{x}_3 - x_3) \\
\dot{\hat{x}}_4 &= \frac{x_2 - \hat{x}_6 - \hat{i}_{loudq}}{C} - \omega_o \hat{x}_3 - 2\lambda(\hat{x}_4 - x_4) \\
\dot{\hat{x}}_5 &= \frac{\hat{x}_3 - R_2 \hat{x}_5 - \hat{V}_{gd}}{L_2} + \omega_o \hat{x}_6 - 2\lambda(\hat{x}_5 - x_5) \\
\dot{\hat{x}}_6 &= \frac{\hat{x}_4 - R_2 \hat{x}_6 - \hat{V}_{gq}}{L_2} - \omega_o \hat{x}_5 - 2\lambda(\hat{x}_6 - x_6) \\
\dot{\hat{i}}_{loadd} &= C\lambda^2(\hat{x}_3 - x_3) \\
\dot{\hat{i}}_{loadq} &= C\lambda^2(\hat{x}_4 - x_4) \\
\dot{\hat{V}}_{gd} &= L_2\lambda^2(\hat{x}_5 - x_5) \\
\dot{\hat{V}}_{gq} &= L_2\lambda^2(\hat{x}_6 - x_6)
\end{aligned} \tag{34}$$

5. SYSTEM STABILITY ANALISIS

We consider the system given by (30)-(31) and we have the following persistent excitation condition is fulfilled

$$\lim_{t\to\infty} \inf \int_0^t W(\tau)^T W(\tau) d\tau \ \rangle\ 0 \tag{35}$$

We define the following Lyapunov function candidate:

$$V = \frac{1}{2}\sum_{i=1}^{6} e_i^2 + \frac{1}{2\gamma_1}\tilde{\theta}_1^2 + \frac{1}{2\gamma_2}\tilde{\theta}_2^2 \tag{36}$$

The time derivation of (33) considering (30)-(31) is

$$\dot{V} = -\sum_{i=1}^{6} k_i e_i^2 \tag{37}$$

Then, we have the following results:

i. The system signals in the closed loop are bounded.
ii. The errors $e_1 = x_5 - x_5^{ref}$ and $e_4 = x_6 - x_6^{ref}$ vanish.
iii. $\hat{\theta}_1$ and $\hat{\theta}_2$ converge, respectively, to their real values θ_1 and θ_2.

Proof

i. Since $V \rangle 0$ and $\dot{V} \langle 0$ then equilibrium $(e, \tilde{\theta}) = 0$ is globally asymptotically stable. Therefore, the state vector $x(t)$ is globally asymptotically stable.
ii. Let F be the set defined as $F = \{(e,\tilde{\theta}) \in IR^5 / e = 0\}$ where $\dot{V} = 0$. We have $(e,\tilde{\theta})$ converges to the largest invariant set M of (30) contained in F according to Lasalle's Invariance theorem. In another words, $e(t) \to 0\ as\ t \to \infty$. Therefore, x_5 and x_6 follow their references.

iii. We prove that $\tilde{\theta}$ converges to zero. That's why we demonstrate by contradiction that the invariant set M is limited to the origin that means $M = \{[0 \quad 0 \quad 0 \quad 0 \quad 0]^T\}$. We suppose $[0 \quad 0 \quad 0 \quad 0 \quad \varepsilon] \in M$ for some

$$\varepsilon \in IR/\{\mathbf{0}\} \qquad (38)$$

Let $\left[e^T(0) \quad \tilde{\theta}\right] = [0 \quad 0 \quad 0 \quad 0 \quad \varepsilon]$, as M is invariant, it follows that for all $t \rangle 0$, $e(t) = 0$ (and so $\dot{e}(t) = 0$), and with (30), we get $W\tilde{\theta} = 0$ for all $t \rangle 0$ (39)

On the other hand, using (31), we have $\dot{\tilde{\theta}} = 0$ and so $\tilde{\theta}(t) = \varepsilon \neq 0$ for all $t \rangle 0$. Now multiplying (39) by W^T and integrating both sides, yields: $\lim_{t\to\infty} \inf \int_0^t W(\tau)^T W(\tau) d\tau)\varepsilon = 0$ which implies that $\varepsilon = 0$ in view of (35). But this contradicts (38). Hence, the invariant set M is reduced to the origin and consequently $(e, \tilde{\theta})$ converges to zero. In particularly, $\tilde{\theta}$ converges to zero.

6. SIMULATION AND DISCUSSION

The VSI, the LC filter, the coupling inductor, the adaptive backstepping controller as well as the high gain observer were modelled using a simulation software in order to evaluate their performances. The simulation parameters are: $R_1 = 0.15\Omega$, $L_1 = 1.5mH$, $C = 45\mu F$, $f = 50\ Hz$, $k_1 = 1000$, $k_2 = 5000$, $k_3 = 1000$, $k_4 = 1000$, $k_5 = 1000$, $k_6 = 5000$, $\gamma_1 = 1e^{-9}$, $\gamma_2 = 1e^{-9}$, $\lambda = 1500$.

The direct component of the current reference (x_5^{ref}) is set to 2A and the quadrature component of the current reference (x_6^{ref}) is set to 0A in order to compensate the local reactive power consumed by the load. At 0.5s, the grid resistance was changed from 0.03 Ω to 0.05 Ω and the grid inductance from 0.2mH to 0.4mH. At 0.75s, the load current was increased.

Fig. 2 shows the output current with its reference. The desired value of the output current is achieved after 0.18s. Besides, the steady state is reached even after the load current and the grid parameters variation. Fig. 3 gives the grid resistance and inductance estimates which follow their real values. In Fig. 4 and Fig. 5, the observed value of the load current and the grid voltage are presented and they converge to their real values.

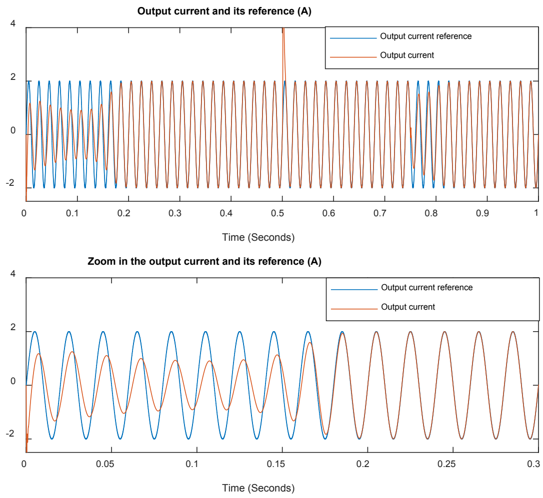

Fig. 2. Output current and its reference

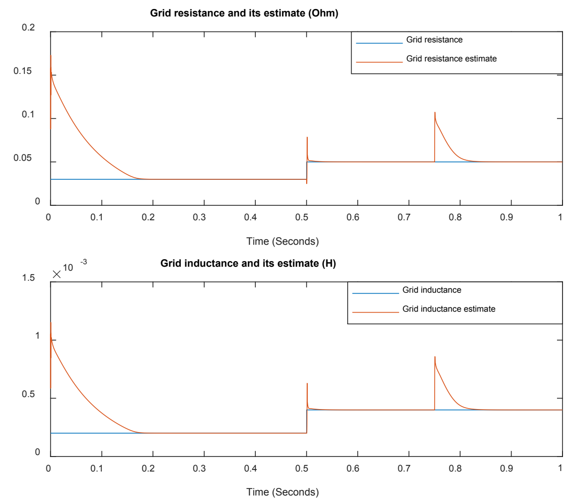

Fig. 3. Grid resistance and inductance with their estimates

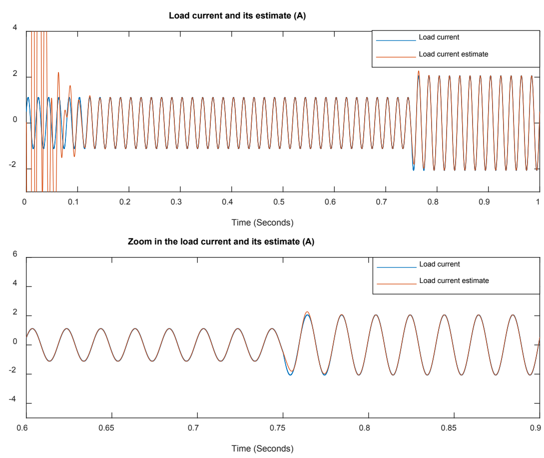

Fig. 4. Load current and its estimate

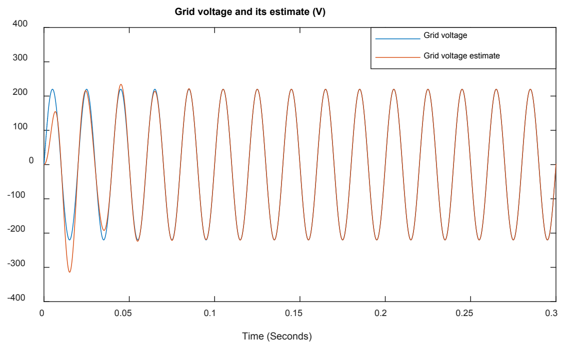

Fig. 5. Grid voltage and its estimate

7. CONCLUSIONS

Firstly, a VSI connected to the main grid through an LC filter and a coupling inductor was modelled. Then, we proposed an adaptive output feedback controller using the backstepping technique and the high gain approach. The backstepping controller has the ability to regulate the injected current and estimate the grid resistance and inductance at the same time. Moreover, the controller compensates the reactive power of the local load by enforcing the quadrature component of the output current to be equal to zero. The high gain observer was designed to estimate the values of the load current and the grid voltage that are unknown and time varying. In that way, we can reduce the sensors number and enhance the system reliability. The behaviour of the adaptive controller combined to the observer was simulated and verified throughout many simulations taking into account the grid parameters and load current variations. Furthermore, the system stability was analysed on the basis of Lyapunov theory.

REFERENCES

Abdmouleh, Z., Gastli, A., Ben-Brahim, L., Haouari, M. and Al-Emadi, N. A. (2017). Review of optimization techniques applied for the integration of distributed generation from renewable energy sources. *Renewable Energy,* 113, 266-280.

Bouzid, M. A., Guerrero, J. M., Cheriti, A., Bouhamida, M., Sicard, P. and Benghanem, M. (2015). A survey on control of electric power distributed generation systems for microgrid applications. Renewable and Sustainable Energy Reviews, 44, 751-766.

Calle-Prado, A., Alepuz, S., Bordonau, J., Nicolas-Apruzzese, J., Cortés, P and Rodriguez, J. (2015). Model Predictive Current Control of Grid-Connected Neutral-Point-Clamped Converters to Meet Low-Voltage Ride-Through Requirements. *IEEE Transactions on Industrial Electronics*, 62 (3). 1503-1514.

Chaabane, M., Farza, M., Ben Abdennour, R., Derbel, N., Zasadzinski, M. and M'Saad, M. (2014). Observer Synthesis for nonlinear systems. *Gabes university & Caen university*.

Farza, M., M'Saad, M. and Rossignol, L. (2004). Observer design for a class of MIMO nonlinear systems. *Automatica*, 40 (1), 135-143.

Hirsch, A., Paraga, Y. and Guerrero, J. (2018). Microgrids: A review of Technologies, Key Drivers, and Outstanding Issues. *Renewable and Sustainable Energy Reviews*, 90, 402-411.

Hornik, T. and Zhong, Q.C. (2011). Current-control strategy for voltage-source inverters in microgrids based on and repetitive control. IEEE Transactions On Power Electronics, 26 (3).

Hossain, M.A., Roy Pota, H., Issa, W. and Hossain, M. J. (2017). Overview of AC Microgrid Controls with Inverter-Interfaced Generations. *Energies,* 10 (9), 1300.

Hu, J., Zhu, J. and Dorrell, D. G. (2013). Model-predictive control of grid-connected inverters for PV systems with flexible power regulation and switching frequency reduction. *2013 IEEE Energy Conversion Congress and Exposition*, 540-546.

Komurcugil, H., Altin, N., Ozdemir, S. and Sefa, I. (2016). Lyapunov-Function and Proportional-Resonant-Based Control Strategy for Single-Phase Grid-Connected VSI With LCL Filter. *IEEE Transactions on Industrial Electronics*, 63 (5), 2838-2849.

Mariam, L., Basu, M. and Conlon, M. F. (2013). A Review of Existing Microgrid Architectures, *Journal of Engineering*, 2013 (937614).

Siddique, A., Munsi, S., Sarker, S. K., Das, S. K. and Islam, R. (2019), Voltage and current control augmentation of islanded microgrid using multifunction model reference modified adaptive PID controller. *International Journal of Electrical Power & Energy Systems*, 113, 492-501.

Zamora, R. and Srivastava, A. K. (2010). Controls for microgrids with storage: Review, challenges, and research needs, *Renewable and Sustainable Energy Reviews*, 14 (7), 2009-2018.